HHS Public Access

Author manuscript

Biochem Pharmacol. Author manuscript; available in PMC 2018 January 15.

Published in final edited form as:

Biochem Pharmacol. 2017 January 15; 124: 94–102. doi:10.1016/j.bcp.2016.11.012.

A Novel Role for PHT1 in the Disposition of L-Histidine in Brain: *In Vitro* Slice and *In Vivo* Pharmacokinetic Studies in Wildtype and *Pht1* Null Mice

Xiao-Xing Wang[a], **Yongjun Hu**[a], **Richard F. Keep**[b], **Noriko Toyama-Sorimachi**[c], and **David E. Smith**[a,*]

[a]Department of Pharmaceutical Sciences, College of Pharmacy, University of Michigan, Ann Arbor, MI, USA

[b]Department of Neurosurgery, University of Michigan Health System, Ann Arbor, MI, USA

[c]Department of Gastroenterology, Research Institute, National Center for Global Health and Medicine, Tokyo, Japan

Abstract

PHT1 (SLC15A4) is responsible for translocating L-histidine (L-His), di/tripeptides and peptide-like drugs across biological membranes. Previous studies have indicated that PHT1 is located in brain parenchyma, however, its role and significance in brain along with effect on the biodistribution of substrates is unknown. In this study, adult gender-matched *Pht1*-competent (wildtype) and *Pht1*-deficient (null) mice were used to investigate the effect of PHT1 on L-His brain disposition via *in vitro* slice and *in vivo* pharmacokinetic approaches. We also evaluated the serum clinical chemistry and expression levels of select transporters and enzymes in the two genotypes. No significant differences were observed between genotypes in serum chemistry, body weight, viability and fertility. PCR analyses indicated that *Pept2* had a compensatory up-regulation in *Pht1* null mice (about 2-fold) as compared to wildtype animals, which was consistent in different brain regions and confirmed by immunoblots. The uptake of L-His was reduced in brain slices by 50% during PHT1 ablation. The L-amino acid transporters accounted for 30% of the uptake, and passive (other) pathways for 20% of the uptake. During the *in vivo* pharmacokinetic studies, plasma concentration-time profiles of L-His were comparable between the two genotypes after intravenous administration. Still, biodistribution studies revealed that, when sampled 5 min after dosing, L-His values were 28–48% lower in *Pht1* null mice, as compared to wildtype animals, in brain parenchyma but not cerebrospinal fluid. These findings suggest that PHT1 may play an important role in histidine transport in brain, and resultant effects on histidine/histamine homeostasis and neuropeptide regulation.

*Corresponding author: UMICH College of Pharmacy, 428 Church Street, Room 4008, Ann Arbor, Michigan 48109-1065, USA; Telephone: +1 734 647 1431; Facsimile: +1 734 615 6162; smithb@umich.edu.

Note: The authors declare no competing financial interest.

Graphical Abstract

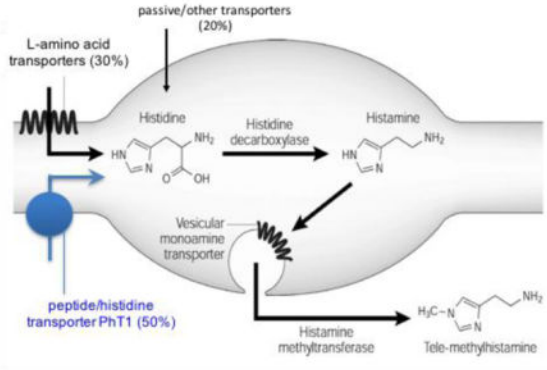

Keywords

PHT1; L-Histidine; Pharmacokinetics; Biodistribution; Brain; Mice

1. Introduction

PHT1 (SLC15A4), a member of the proton-coupled oligopeptide transporter (POT) superfamily, is responsible for translocating various di/tripeptides and peptide-like drugs across biological membranes, as well as the amino acid L-histidine [1]. Unlike two other peptide transporters, PEPT1 (SLC15A1) and PEPT2 (SLC15A2), which have been well studied, there is little known about PHT1 expression, localization, function and pharmacological relevance. PHT1 is abundantly found in the brain and eye [2,3]. PHT1 has an age-dependent increase in brain expression [4], similar to the changes found in the histaminergic system [5–9]. In contrast, PEPT2 shows an age-dependent decrease in brain expression and PHT1 function dominated in the uptake of a dipeptide in brain slices from adult rodents, suggesting a significant role in regulating both endogenous and exogenous L-histidine (L-His) and peptides/mimetics in brain [4]. PHT1 transcripts are also detected in rat thyroid gland [10] and skeletal muscle [11]. A recent study showed that PHT1 and PHT2 are involved in the immune response [12]. These authors reported that PHTs were preferentially expressed in dendritic cells, located at endosomes and lysosomes, mediating the release of bacterially derived components into the cytosol.

L-Histidine (L-His) is one of the proteinogenic amino acids, which is obtained from dietary metabolism and protein turnover [13]. L-His possesses several crucial biological functions, including formation of the myelin sheath, detoxification of heavy metals, and the manufacturing of white and red blood cells. It is also a precursor of histamine, carnosine, ergothioneine, and vitamin C [14]. Studies on the transport of L-His in brain would extend our understanding of neuropeptide regulation, histamine homeostasis, and potential targets for drug delivery to neuronal and non-neuronal cells. In the central nervous system (CNS), major transporters for L-His include the Na^+-coupled neutral amino acid transporters (e.g., SNATs, which belong to the SLC38 family) [15,16], Na^+-independent amino acid transporters (e.g., LATs and CATs, which belong to the SLC7 family) [17,18], some

members of the Na^+-and Cl^--dependent neurotransmitter transporter family (e.g., B^0AT2 and NTT4, which belong to the SLC6 family) [19–21], as well as the peptide/histidine transporters (e.g., PHT1 and PHT2, which belong to the SLC15 family) [4,22].

Histamine, one of the most important metabolites of L-His, is formed in the brain during catalysis by histidine decarboxylase (HDC). While much of the research effort has focused on the enzymatic production of histamine via HDC, little attention has been paid to the mechanism by which L-His gains entry into neurons. Due to its polarity and lack of a transport system, histamine cannot pass through the barrier systems of the brain [23]. Moreover, the availability of its precursor, L-His, is positively correlated with brain histamine production and, consequently the regulatory functions of histamine [24,25]. Significant changes in brain histamine levels have been observed in several neurological diseases, such as multiple sclerosis, Alzheimer's disease, Down's syndrome and Wernicke's encephalopathy [26]. Dysfunction of HDC and the L-His transporters in brain may be related to these neurological disorders.

In the present study, we hypothesized that PHT1 ablation would substantially reduce the uptake of L-His in the brain of adult mice. Initial phenotypic analyses were performed in *Pht1*-competent (wildtype) and *Pht1*-deficient (null) mice, along with gene expression levels of POTs and select transporter/enzyme proteins. Subsequent studies evaluated the functional activity of PHT1 by studying the *in vitro* uptake of L-His in regional brain slices, and the *in vivo* pharmacokinetics and biodistribution of L-His after intravenous administration.

2. Materials and methods

2.1. Chemicals

L-[^{3}H]histidine (500 mCi/mmol), L-[^{14}C]histidine (322 mCi/mmol), [^{14}C]mannitol (53 mCi/mmol) and [^{3}H]dextran-70,000 (110 mCi/mg) were purchased from American Radiolabeled Chemicals (St. Louis, MO). Unlabeled L-histidine, mannitol and dextran-70,000 were purchased from Sigma-Aldrich (St. Louis, MO). Protease inhibitor cocktail was purchased from Roche (Seattle, WA). Power SYBR Green PCR Master Mix was purchased from Applied Biosystems (Foster City, CA). All other chemicals were obtained from standard sources.

2.2. Animals

Gender- and age-matched *Pht1*-competent (wildtype or $Pht1^{+/+}$) and *Pht1*-deficient (null or $Pht1^{-/-}$) mice, 7–10 weeks old, were used in this study [27]. PCR analysis, using genomic DNA isolated from tail biopsies, was performed to confirm the subsequent production of *Pht1* null mice. The *Pht1* gene had a forward primer 5′-GATCGAGGTCCAGAAGCCACTCG-3′ and a reverse primer 5′-GAGTTGTGTCACTCACCCACTTCT-3′. The Neo gene, inserted during homologous recombination in *Pht1* null mice, had a forward primer 5′-GGAGAGGCTATTCGGCTATG-3′ and a reverse primer 5′-GCTCTTCAGCAATATCACGG-3′. All animals were bred on a C57BL/6 background (≥ 99%). The mice were housed in a temperature-controlled environment with 12 h light and

dark cycles, and received a standard diet and water ad libitum (Unit of Laboratory Animal Medicine, University of Michigan, Ann Arbor, MI). All mouse studies were performed in accordance with the Guide for the Care and Use of Laboratory Animals as adopted and promulgated by the U.S. National Institutes of Health.

2.3. Initial phenotypic analyses

Pht1 null mice were evaluated for body weight and serum clinical chemistry in comparison to those of wildtype mice (by Animal Diagnostic Core, ULAM, University of Michigan, Ann Arbor, MI), as described previously for *Pept1* null mice [28]. Viability and fertility were also monitored.

2.4. Gene and protein expression

Quantitation of POTs (*Pept1*, *Pept2*, *Pht1* and *Pht2*), select amino acid transporters (*Lat1*, *Snat1*, *Snat3* and *Ntt4*) and histidine decarboxylase (*Hdc*) was performed in several tissues of adult wildtype and *Pht1* null mice using a 7300 Real-Time PCR system (Applied Biosystems, Foster City, CA) [29]. Tissues of interest included cerebral cortex, cerebellum, hippocampus, hypothalamus and choroid plexus. In brief, 2.0 μg of total RNA, isolated using the RNeasy Plus Mini Kit (Qiagen, Valencia, CA), was reverse-transcribed into cDNA using the Omniscript RT Kit (Qiagen, Valencia, CA) with 16-mer random primers. The mouse *Gapdh* gene was used as an internal control of cDNA quality and quantity. The primers were designed using Primer 3.0 (Applied Biosystems, Foster City, CA) and synthesized by Integrated DNA Technologies (Coraville, IA) (Table 1). The real-time PCR thermal conditions were 1 cycle at 50 °C for 2 min, 1 cycle at 95 °C for 10 min, 40 cycles at 95 °C for 15 s and then 60 °C for 1 min. The ΔCT method was used to calculate the relative levels of target gene transcripts in mice, where the ratio of target gene to *Gapdh* was equal to $2^{-\Delta CT}$, ΔCT = CT(gene) − CT(Gapdh).

Immunoblot analysis was performed for PEPT2 protein, as described previously with minor changes [30]. Tissue lysis buffer consisted of neuronal protein extraction reagent (Thermo Scientific, Rockford, IL) with the addition of proteinase inhibitor cocktail. Kidney protein served as positive control for PEPT2 [31].

2.5. In vitro uptake of L-His in regional brain slices

Adult wildtype and *Pht1* null mice were used to evaluate the contribution of PHT1 in L-His uptake. Brain slices, prepared using a method described previously [4], were incubated in buffer containing 2 μM [^{3}H]L-His (0.1 μCi) and [^{14}C]mannitol (0.05 μCi). The incubation was performed in a chamber filled with artificial cerebrospinal fluid (aCSF) buffer at 37°C, which was continuously bubbled with 5% CO_2 and 95% O_2. The aCSF buffer consisted of (mM): 127 NaCl, 20 $NaHCO_3$, 2.4 KCl, 0.5 KH_2PO_4, 1.1 $CaCl_2$, 0.85 $MgCl_2$, 0.5 Na_2SO_4 and 5.0 glucose (pH 7.4). Incubation times were 1, 3, 5 and 10 min, after which time 1.5 mL ice-cold aCSF buffer was added to the chamber to terminate the reaction. The samples were immediately filtered through 100 μm nylon mesh and then washed five times with 1.5 mL ice-cold aCSF buffer. The filter (and tissue slices) were transferred to a scintillation vial containing 0.33 mL hyamine hydroxide and left overnight at 37°C to dissolve the tissue. The samples were then mixed with a 7.0-mL aliquot of Cytoscint cocktail (MP Biomedicals,

Solon, OH). Radioactivity was measured using a Beckman LS 6000 SC dual-channel liquid scintillation counter (Beckman Coulter Inc., Fullerton, CA).

The uptake of L-His in brain slices was determined using the following equation [32]:

$$Histidine\ Uptake = \frac{(Histidine_t - Histidine_f) - (Mannitol_t - Mannitol_f) \times \frac{Histidine_{media}}{Mannitol_{media}}}{Tissue\ Weight \times Histidine_{media}}$$

where *uptake* was calculated as μL/mg wet tissue weight. The subscript *t* represents the total radioactivity, *f* the filter-binding and *media* the amount of drug in the incubation media.

To further investigate the contribution of amino acid transporters on L-His uptake, as well as the substrate specificity of PHT1, excess amounts (5 mM) of L-His, L-glutamine, L-leucine, L-asparagine or BCH (2-amino-2-norbornanecarboxylic acid) were added as inhibitors of the amino acid transporters. Similarly, dipeptides (glycylsarcosine and carnosine) were used as inhibitors of the peptide transporters. These studies were performed on hypothalamus slices following a 3-min incubation period.

2.6. In vivo pharmacokinetics and biodistribution of L-His

L-His solutions were prepared by mixing appropriate amounts of [^{14}C]labeled and unlabeled L-His in normal saline to reach the desired dose of 1 nmol/g (0.4 μCi/mouse). A 100-μL volume of solution was administrated by tail vein injection. Serial blood samples (15–20 μL), obtained via tail nicks, were then collected at 0.5, 1, 2, 5, 10, 15, 20 and 30 min after the intravenous dose. Blood samples were collected in 0.2-mL microcentrifuge tubes containing heparin. Heparinized blood samples were centrifuged immediately at 3000 g for 3 min at ambient temperature. A 5- to 10-μl aliquot of plasma was then mixed with 6.0 mL of Cytoscint cocktail. Radioactivity was measured using a dual-channel liquid scintillation counter.

A single CSF sample (5 μL) was obtained from the cisterna magna of each mouse at 2, 5, 10, 20 and 30 min after dosing. The mouse was euthanized and decapitated, and select tissues of brain (e.g. cerebral cortex, cerebellum, hypothalamus and hippocampus) were then isolated, blotted dry and weighed. The samples were dissolved in 330 μL of 1 M hyamine hydroxide and incubated overnight at 37°C. An intravenous bolus injection of [^{3}H]dextran-70,000 (0.25 μCi/mouse) was administered just prior to harvesting the tissue samples to correct for the vascular space.

A noncompartmental pharmacokinetic analysis of L-His was performed on the plasma concentrations of L-His after intravenous bolus dosing using Phoenix/WinNonlin version 6.4 (Pharsight Inc. Mountain View, CA). Total area under the plasma concentration-time curve (AUC) was calculated using the trapezoidal rule. Clearance (CL), volume of distribution (V_{ss}), half-life ($t_{1/2}$), terminal disposition rate constant (λ_z) and mean residence time (MRT) were calculated using standard methods.

2.7. Statistics

All the experimental results were reported as mean ± SE. A two-tailed unpaired Student's t-test was applied when comparing statistical differences between two treatment groups. For multiple comparisons, one-way analysis of variance (ANOVA) was used followed by Tukey's test for pairwise comparisons between all the treatment groups. A p value ≤ 0.05 was considered significant. All linear and nonlinear regressions were performed by Prism v5.0 (GraphPad Software, Inc., La Jolla, CA).

3. Results

3.1. Identification and initial phenotypic analyses of Pht1 null mice

These studies were performed to test for obvious differences in fundamental characteristics between the two mouse genotypes. In this regard, PCR analyses of genomic DNA extracted from tail biopsies demonstrated that *Pht1* genomic DNA was present in wildtype but not *Pht1* null mice (Fig. 1). Since *Pht1* null primers were designed specifically to target the *Neo* gene, a band was observed in *Pht1* null mice but not in wildtype animals. No obvious behavioral abnormality was observed in *Pht1* null mice when compared with wildtype animals. *Pht1* null mice were fertile and appeared healthy. There were no significant differences between genotypes in body weight or in any of the serum clinical chemistry values (Table 2).

3.2. Gene and protein expression

The purpose of these studies was to determine if *Pht1* mice were different, as compared to wildtype animals, in their gene expression of POT family members and other relevant transporters and enzymes. Protein expression for a particular transporter was also performed in select cases. PCR analyses in wildtype mice indicated that *Pht1* was expressed, along with *Pept2*, in the cerebral cortex, cerebellum, hypothalamus, hippocampus and choroid plexus (Fig. 2). Interestingly, *Pept2* showed a compensatory up-regulation in *Pht1* null mice (about 2-fold), which was consistently observed in the different brain regions. Expression of other peptide transporters (*Pept1* and *Pht2*) and *Hdc* were comparable between the two genotypes. Some of the amino acid transporters had different transcription levels between genotypes, however, there was no consistent pattern in the different brain regions. The upregulation of *Pept2* in *Pht1* null mouse brain was confirmed by immunoblot analysis (Fig. 3). PEPT2 protein could be detected in different brain regions, in which expression was increased about 2-fold in the cerebral cortex, hippocampus and hypothalamus of *Pht1* null mice as compared to wildtype animals.

3.3. In vitro uptake of L-His in regional brain slices

These studies were performed to examine if regional functional activity, along with substrate specificity, differed between wildtype and *Pht1* null mice in the brain uptake of a model substrate, L-His, using an *in vitro* model. L-[^{3}H]His uptake was linearly correlated with time over the first 3–10 min, with no consistent trend for either genotype or regional brain slice (Fig. 4A–D). As a result, 3-min uptakes were used to estimate the initial rates of L-His, which were reduced by 37–60% during PHT1 ablation depending upon the regional brain

slice studied (Fig. 4E). To assess the substrate specificity of PHT1, the 3-min uptake of L-[^{3}H]His was evaluated in hypothalamus by inhibition studies (Fig. 5). In wildtype mice, the uptake of L-His was reduced to 20% of normal by the amino acids L-histidine, L-glutamine, L-lysine and L-asparagine, and to 45–72% of normal by the dipeptides glycylsarcosine and carnosine (5 mM each). In contrast, residual uptake values of L-His in *Pht1* null mice were similar between control animals (L-His alone) and in the presence of dipeptides. In the presence of amino acids, values for L-His uptake were significantly reduced in *Pht1* null mice, and similar between the two genotypes. Finally, in comparing control values, the uptake of L-His in *Pht1* null mice was 50% of that observed in wildtype animals.

3.4. In vivo pharmacokinetics and biodistribution of L-His

These studies were designed to evaluate whether or not the *in vivo* distribution of a model Pht1 substrate, L-His, was different between genotypes with respect to its systemic plasma exposure, accumulation in regional brain sections and CSF concentrations. In this regard, we found that the plasma concentration-time profiles of L-[^{14}C]His after intravenous injection were comparable in wildtype and *Pht1* null mice (Fig. 6). As a result, the pharmacokinetic properties of L-His were not different between the two genotypes, as judged by noncompartmental analyses (Table 3). Still, biodistribution studies in brain revealed that L-His values were 28–48% lower in *Pht1* null mice, as compared to wildtype animals, in the cerebral cortex, cerebellum, hippocampus and hypothalamus, but not CSF, when sampled 5 min after dosing (Fig. 7).

4. Discussion

Compared with PEPT1 and PEPT2, little is known about the expression, localization, function and pharmacological relevance of PHT1, another member of the SLC15 family. Based on limited previous reports [2,4], PHT1 protein was expressed in the brain and retina of rat, and showed high affinity for L-His in *Pht1*-transfected Xenopus laevis oocytes [2]. PHT1 protein was also expressed in the brain of adult but not neonatal rats and mice, showing a dominant role in glycylsarcosine brain uptake in adult rodents [4]. However, the significance of PHT1 in uptake of its amino acid substrate, L-His, in brain was not evaluated in these studies [4]. Thus, the *in vitro* brain slice and *in vivo* pharmacokinetic/biodistribution studies proposed here for L-His in brain are a good starting point from which to understand the role and significance of PHT1 in neuropeptide regulation, histamine homeostasis, and the potential for targeted drug delivery to neuronal and non-neuronal cell types.

Several novel findings were revealed through phenotypic analyses, *in vitro* brain slice uptake incubation and *in vivo* pharmacokinetic studies in wildtype and *Pht1* null mice. Specifically: 1) *Pht1* null mice displayed no obvious phenotype and had serum clinical chemistry values that were comparable to wildtype mice; 2) PHT1 was expressed, along with PEPT2, in the brain parenchyma (cortex, cerebellum, hippocampus and hypothalamus) of wildtype mice; 3) the mRNA and protein levels of PEPT2 were significantly up-regulated in *Pht1* null mouse brain, suggesting a compensatory role of PEPT2 in these mice; 4) the uptake of L-[^{3}H]His was about 50% lower in *Pht1* null mouse brain slices as compared to those from wildtype mice, indicating that PHT1 makes a significant contribution towards L-His uptake

into brain parenchyma; 5) the uptake of L-[^{3}H]His could be inhibited by dipeptides and, in addition to L-His, by several other amino acids; and 6) PHT1 deficiency did not affect the *in vivo* systemic exposure of L-[^{14}C]His in plasma or CSF, but reduced its distribution into brain parenchyma during the first 5 min of intravenous dosing. These findings suggest that PHT1 may play an important role in L-His transport and, perhaps, in histidine-histamine homeostasis in the brain.

The results in Fig. 5 indicated there were key differences (and similarities) in the inhibition profiles of wildtype and *Pht1* null mice. For example, in comparing the inhibition studies in wildtype mice alone, the amino acids (except for leucine) reduced the uptake of L-His to about 20% of control, whereas the dipeptides reduced L-His uptake to 40–65% of control (all changes were significant). These profiles reflected the collective contributions of PHT1, amino acid transporters and nonsaturable/passive pathways for the uptake of L-His in wildtype mice. In comparing the inhibition studies in *Pht1* null mice alone, the same amino acids resulted in significant changes from control, however, L-His uptake in the presence of dipeptides was not significantly different. Most importantly, the control value in *Pht1* null mice was only 50% of the control value in wildtype mice, indicating a major influence of PHT1 in the uptake of L-His. Thus, these profiles reflected the collective contributions of amino acid transporters and nonsaturable/passive pathways for the uptake of L-His in the absence of PHT1. Overall, the combined mechanisms for L-His uptake in brain (hypothalamus) were PHT1 (50%), amino acid transporters (30%) and nonsaturable/passive processes (20%).

Of the POTs, PEPT2 is expressed in the brain of adult rats, especially in epithelial cells of the choroid plexus [30]. The brain expression of PEPT2 is maximal in the fetus, declining with age to 14% of those levels in the adult brain. In contrast, the expression and function of PHT1 protein gradually increases with age, agreeing with its function as indicated by the uptake of glycylsarcosine in adult rodent brain slices [4]. Another POT, PHT2 can also recognize L-His as a substrate, but this transporter is barely detected in brain [3,4], as is PEPT1 [30]. The effect of *Pht1* depletion on the transcription of those other POTs, amino acid transporters and related enzymes, as well as on the total brain entry of L-His was unknown and the present study was able to address this with the availability of *Pht1* null mice [27,33]. PEPT2 protein was up-regulated in different brain regions of *Pht1* null mice, which may suggest a compensatory role of PEPT2 as a transporter for di/tripeptides in brain (Fig. 3). This was not observed in other tissues, such as kidney, testis, lung, intestine, spleen or colon (data not shown). As expected, there was no gene expression of *Pept1* or *Pht2* in the brain of both genotypes, which was consistent with previous studies in wildtype rodents [4]. Interestingly, in rat synaptosomes prepared from cerebral cortex [34], the uptake of L-His (2 μM) was not inhibited by GlySar (2.5 mM) nor was the uptake of GlySar (20 μM) inhibited by L-His (2.5 mM). Thus, the functional data of Fujita et al. [34] in synaptosomes suggest that, although PHT1 expression will not be synaptic, its expression may reflect a cell body or axonal distribution in neurons.

Although brain barrier systems determine the concentration of amino acids in CSF and extracellular fluid (ECF), transporters expressed on the membranes of brain parenchyma cells also participate in the regulation of intracellular fluid homeostasis [35]. More

importantly, transporters in brain parenchyma are responsible for the translocation of metabolic substrates, neurotransmitters and neurotransmitter precursors, which can regulate signaling pathways [36]. Amino acid transporters of L-His in brain parenchyma include the Na^+-dependent neutral amino acid transporters (SNATs, SLC38 family) [15,16], some members of the sodium- and chloride-dependent neurotransmitter transporter family (SLC6 family) (e.g. B^0AT2, and NTT4) [19–21], Na^+-independent amino acid transporters (e.g. LATs and CATs, belong to SLC7 family) [17,18], and the peptide/histidine transporter PHT1 [4,22]. Among the amino acid transporters tested in the present study, NTT4, SNAT1 and SNAT3 showed extensive transcription. SNATs have a very broad tissue distribution and are responsible for the net flux of amino acids in CNS [15,37]. The major physiological function of SNATs in the central nervous system is to transport glutamine in the glutamate/glutamine cycle [38]. Affinity of SNATs to L-His is relatively low, with Michaelis-Menten (K_m) values in the millimolar range [39–41]. NTT4 (SLC6A17) is identified only in the nervous system, especially in synaptic vesicles [42], with a Km of 1–2 mM for proline and glycine and interestingly no affinity for L-His [43].

Another important consideration was that of differences in the gene expression of amino acid transporters in wildtype and *Pht1* null mice. In this regard, there appeared to be no consistent pattern of change in either a specific amino acid transporter or brain region with respect to the up-/down-regulation between genotypes. Using hypothalamus as an example, since the *in vitro* inhibition studies were performed in this brain region along with *in vivo* studies, the only amino acid transporter that showed a statistically significant difference was Ntt4, with gene expression being reduced by only 12% (Fig. 2). However, in *Pht1* null mice, the *in vivo* uptake of L-His was reduced 2-fold relative to the values observed in wildtype animals (Fig. 6). Moreover, similar reductions in the *in vivo* L-His uptake were observed in other brain regions even though Ntt4 gene expression increased 2-fold in cortex, had no change in cerebellum, and was reduced only 20% in hippocampus. These findings make it unlikely that changes in the gene expression of amino acid transporters can explain the differences in transport acitivity of L-His during *Pht1* ablation. Still, it would be important to measure, in future studies, if protein expression had also changed.

PHT1 made a significant contribution towards L-His disposition in brain slices. With PHT1 ablation, L-His uptake was reduced by 50% *in vitro* during 3-min brain slice incubations, and by 28–48% *in vivo* in brain regions after intravenous dosing. The rat PHT1 isoform is a high affinity transporter, as judged by a K_m = 17 μM for L-His uptake in oocytes expressing PHT1 protein [2]. As shown in Fig. 5, the transport of L-His by PHT1 could be inhibited, as expected, by dipeptides (e.g., carnosine and glycylsarcosine) and excess L-His. However, an interesting finding was that some amino acids (not including L-leucine) and a system L-amino acid transport inhibitor, BCH, substantially reduced the uptake of L-His via PHT1. This phenomenon has not been reported previously. Therefore, the interaction between amino acids with positive (L-His, L-lysine) or uncharged polar (L-asparagine, L-glutamine) side chains and PHT1 needs further investigation to test whether other amino acids, in addition to L-His, are substrates for PHT1.

An effect of PHT1 ablation on the brain disposition of L-His was also found *in vivo* with a 28–48% reduction into uptake into brain regions after intravenous dosing (Fig. 7). These

results suggest a role of PHT1 at the blood-brain barrier. Carl et al. [44] reported the protein expression of PHT1 in hCMEC/D3 cells, an immortalized human brain endothelial cell line commonly used for *in vitro* blood-brain barrier studies. Those cells showed some evidence of polarized L-His and carnosine (a dipeptide) transport. The role of PHT1 in di/tripeptide, peptidomimetic and amino acid transport at the blood-brain barrier merits further investigation.

In this study, no obvious phenotype was observed when comparing the body weight, fertility, serum clinical chemistry and routine behavior of wildtype and *Pht1* null mice. Indeed, this observation is not unusual during transporter ablation and, often times, requires that the animals be challenged by a certain stress (e.g., drug, chemical or disease state). This scenario was clearly demonstrated by the death of *Mdr1(−/−)* knockout mice during ivermectin exposure [45] and by the phototoxic ear lesions observed in *Bcrp1(−/−)* knockout mice when fed a diet containing alfalfa [46]. Increased neurotoxicity was also observed in *Pept2(−/−)* knockout mice given chronic administration of the heme precursor 5-aminolevulinic acid [47] as well as increased analgesia in *Pept2(−/−)* knockout mice given the endogenous neuropeptide L-kyotorphin [48]. While this study represents an analysis of L-His disposition in the brain of wildtype and *Pht1* null mice, as evaluated by *in vitro* brain slices and *in vivo* biodistribution studies, these results allow us to explore subsequently if these kinetic differences will translate into pharmacological and/or pathological differences. Still, in their initial study using wildtype and *Pht1* null mice, Sasawatari et al. [27] reported that PHT1 promoted a dextran sodium sulfate-induced colitis through its interaction with Toll-like receptor 9 and NOD1-dependent innate immune responses.

Taken as a whole, it appears that PHT1 accounted for 50% of the total uptake of L-His in brain slices and L-amino acid transporters for 30% of the uptake. In addition, PHT1 ablation significantly affected the *in vivo* blood to brain distribution of L-His. These findings are the first of their kind and suggest that PHT1 plays an important role in histidine transport and perhaps drug delivery to neuronal and non-neuronal cell types.

Acknowledgments

This work was supported by the National Institutes of Health National Institute of General Medical Sciences grant R01-GM115481 (to D.E.S.). Xiao-Xing Wang was supported, in part, by a Rackham Barbour Scholarship from the University of Michigan.

References

1. Smith DE, Clemencon B, Hediger MA. Proton-coupled oligopeptide transporter family SLC15: physiological, pharmacological and pathological implications. Mol Aspects Med. 2013; 34(2–3): 323–36. [PubMed: 23506874]
2. Yamashita T, Shimada S, Guo W, Sato K, Kohmura E, Hayakawa T, Takagi T, Tohyama M. Cloning and functional expression of a brain peptide/histidine transporter. J Biol Chem. 1997; 272(15): 10205–11. [PubMed: 9092568]
3. Sakata K, Yamashita T, Maeda M, Moriyama Y, Shimada S, Tohyama M. Cloning of a lymphatic peptide/histidine transporter. Biochem J. 2001; 356(Pt 1):53–60. [PubMed: 11336635]
4. Hu Y, Xie Y, Keep RF, Smith DE. Divergent Developmental Expression and Function of the Proton-Coupled Oligopeptide Transporters PepT2 and PhT1 in Regional Brain Slices of Mouse and Rat. J Neurochem. 2014; 129(6):955–965. [PubMed: 24548120]

5. Martres MP, Baudry M, Schwartz JC. Histamine synthesis in the developing rat brain: evidence for a multiple compartmentation. Brain Res. 1975; 83(2):261–75. [PubMed: 1109298]
6. Reiner PB, Semba K, Fibiger HC, McGeer EG. Ontogeny of histidine-decarboxylase-immunoreactive neurons in the tuberomammillary nucleus of the rat hypothalamus: time of origin and development of transmitter phenotype. J Comp Neurol. 1988; 276(2):304–11. [PubMed: 3220985]
7. Subramanian N, Whitmore WL, Seidler FJ, Slotkin TA. Ontogeny of histaminergic neurotransmission in the rat brain: concomitant development of neuronal histamine, H-1 receptors, and H-1 receptor-mediated stimulation of phospholipid turnover. J Neurochem. 1981; 36(3):1137–41. [PubMed: 6259281]
8. Tran VT, Freeman AD, Chang RS, Snyder SH. Ontogenetic development of histamine H1-receptor binding in rat brain. J Neurochem. 1980; 34(6):1609–13. [PubMed: 6103919]
9. Toledo A, Sabria J, Rodriguez R, Brandner R, Rodriguez J, Palacios JM, Blanco I. Properties and ontogenic development of membrane-bound histidine decarboxylase from rat brain. J Neurochem. 1988; 51(5):1400–6. [PubMed: 3171585]
10. Romano A, Barca A, Kottra G, Daniel H, Storelli C, Verri T. Functional expression of SLC15 peptide transporters in rat thyroid follicular cells. Mol Cell Endocrinol. 2010; 315(1–2):174–81. [PubMed: 19913073]
11. Everaert I, De Naeyer H, Taes Y, Derave W. Gene expression of carnosine-related enzymes and transporters in skeletal muscle. Eur J Appl Physiol. 2013; 113(5):1169–79. [PubMed: 23124893]
12. Nakamura N, Lill JR, Phung Q, Jiang Z, Bakalarski C, de Maziere A, Klumperman J, Schlatter M, Delamarre L, Mellman I. Endosomes are specialized platforms for bacterial sensing and NOD2 signalling. Nature. 2014; 509(7499):240–4. [PubMed: 24695226]
13. Kopple JD, Swendseid ME. Evidence that histidine is an essential amino acid in normal and chronically uremic man. J Clin Invest. 1975; 55(5):881–91. [PubMed: 1123426]
14. Stifel FB, Herman RH. Histidine metabolism. Am J Clin Nutr. 1971; 24(2):207–17. [PubMed: 4925814]
15. Schioth HB, Roshanbin S, Hagglund MG, Fredriksson R. Evolutionary origin of amino acid transporter families SLC32, SLC36 and SLC38 and physiological, pathological and therapeutic aspects. Mol Aspects Med. 2013; 34(2–3):571–85. [PubMed: 23506890]
16. Hagglund MG, Sreedharan S, Nilsson VC, Shaik JH, Almkvist IM, Backlin S, Wrange O, Fredriksson R. Identification of SLC38A7 (SNAT7) protein as a glutamine transporter expressed in neurons. J Biol Chem. 2011; 286(23):20500–11. [PubMed: 21511949]
17. Usui T, Kubo Y, Akanuma S, Hosoya K. Beta-alanine and l-histidine transport across the inner blood-retinal barrier: potential involvement in L-carnosine supply. Exp Eye Res. 2013; 113:135–42. [PubMed: 23773890]
18. Broer A, Wagner CA, Lang F, Broer S. The heterodimeric amino acid transporter 4F2hc/y+LAT2 mediates arginine efflux in exchange with glutamine. Biochem J. 2000; 349(Pt 3):787–95. [PubMed: 10903140]
19. Fredriksson R, Nordstrom KJ, Stephansson O, Hagglund MG, Schioth HB. The solute carrier (SLC) complement of the human genome: phylogenetic classification reveals four major families. FEBS Lett. 2008; 582(27):3811–6. [PubMed: 18948099]
20. Hagglund MG, Hellsten SV, Bagchi S, Ljungdahl A, Nilsson VC, Winnergren S, Stephansson O, Rumaks J, Svirskis S, Klusa V, Schioth HB, Fredriksson R. Characterization of the transporter B0AT3 (Slc6a17) in the rodent central nervous system. BMC Neurosci. 2013; 14:54. [PubMed: 23672601]
21. Hagglund MG, Roshanbin S, Lofqvist E, Hellsten SV, Nilsson VC, Todkar A, Zhu Y, Stephansson O, Drgonova J, Uhl GR, Schioth HB, Fredriksson R. B(0)AT2 (SLC6A15) is localized to neurons and astrocytes, and is involved in mediating the effect of leucine in the brain. PLoS One. 2013; 8(3):e58651. [PubMed: 23505546]
22. Bhardwaj RK, Herrera-Ruiz D, Eltoukhy N, Saad M, Knipp GT. The functional evaluation of human peptide/histidine transporter 1 (hPHT1) in transiently transfected COS-7 cells. Eur J Pharm Sci. 2006; 27(5):533–42. [PubMed: 16289537]

23. Schwartz JC, Arrang JM, Garbarg M, Pollard H, Ruat M. Histaminergic transmission in the mammalian brain. Physiol Rev. 1991; 71(1):1–51. [PubMed: 1846044]
24. Yoshimatsu H, Chiba S, Tajima D, Akehi Y, Sakata T. Histidine suppresses food intake through its conversion into neuronal histamine. Exp Biol Med (Maywood). 2002; 227(1):63–8. [PubMed: 11788786]
25. Vaziri P, Dang K, Anderson GH. Evidence for histamine involvement in the effect of histidine loads on food and water intake in rats. J Nutr. 1997; 127(8):1519–26. [PubMed: 9237947]
26. Haas HL, Sergeeva OA, Selbach O. Histamine in the nervous system. Physiol Rev. 2008; 88(3): 1183–241. [PubMed: 18626069]
27. Sasawatari S, Okamura T, Kasumi E, Tanaka-Furuyama K, Yanobu-Takanashi R, Shirasawa S, Kato N, Toyama-Sorimachi N. The solute carrier family 15A4 regulates TLR9 and NOD1 functions in the innate immune system and promotes colitis in mice. Gastroenterology. 2011; 140(5):1513–25. [PubMed: 21277849]
28. Hu Y, Smith DE, Ma K, Jappar D, Thomas W, Hillgren KM. Targeted disruption of peptide transporter Pept1 gene in mice significantly reduces dipeptide absorption in intestine. Molecular pharmaceutics. 2008; 5(6):1122–30. [PubMed: 19434858]
29. Hu Y, Xie Y, Wang Y, Chen X, Smith DE. Development and Characterization of a Novel Mouse Line Humanized for the Intestinal Peptide Transporter PEPT1. Molecular pharmaceutics. 2014
30. Shen H, Smith DE, Keep RF, Brosius FC 3rd. Immunolocalization of the proton-coupled oligopeptide transporter PEPT2 in developing rat brain. Molecular pharmaceutics. 2004; 1(4):248–56. [PubMed: 15981584]
31. Shen H, Smith DE, Yang T, Huang YG, Schnermann JB, Brosius FC 3rd. Localization of PEPT1 and PEPT2 proton-coupled oligopeptide transporter mRNA and protein in rat kidney. Am J Physiol. 1999; 276(5 Pt 2):F658–65. [PubMed: 10330047]
32. Teuscher NS, Novotny A, Keep RF, Smith DE. Functional evidence for presence of PEPT2 in rat choroid plexus: studies with glycylsarcosine. The Journal of pharmacology and experimental therapeutics. 2000; 294(2):494–9. [PubMed: 10900224]
33. Kobayashi T, Shimabukuro-Demoto S, Yoshida-Sugitani R, Furuyama-Tanaka K, Karyu H, Sugiura Y, Shimizu Y, Hosaka T, Goto M, Kato N, Okamura T, Suematsu M, Yokoyama S, Toyama-Sorimachi N. The histidine transporter SLC15A4 coordinates mTOR-dependent inflammatory responses and pathogenic antibody production. Immunity. 2014; 41(3):375–88. [PubMed: 25238095]
34. Fujita T, Kishida T, Wada M, Okada N, Yamamoto A, Leibach FH, Ganapathy V. Functional characterization of brain peptide transporter in rat cerebral cortex: identification of the high-affinity type H^+/peptide transporter PEPT2. Brain Res. 2004; 997(1):52–61. [PubMed: 14715149]
35. O'Kane RL, Hawkins RA. Na+-dependent transport of large neutral amino acids occurs at the abluminal membrane of the blood-brain barrier. Am J Physiol Endocrinol Metab. 2003; 285(6):E1167–73. [PubMed: 12933350]
36. He L, Vasiliou K, Nebert DW. Analysis and update of the human solute carrier (SLC) gene superfamily. Hum Genomics. 2009; 3(2):195–206. [PubMed: 19164095]
37. Reimer RJ, Chaudhry FA, Gray AT, Edwards RH. Amino acid transport system A resembles system N in sequence but differs in mechanism. Proc Natl Acad Sci U S A. 2000; 97(14):7715–20. [PubMed: 10859363]
38. Conti F, Melone M. The glutamine commute: lost in the tube? Neurochem Int. 2006; 48(6–7):459–64. [PubMed: 16517023]
39. Nakanishi T, Sugawara M, Huang W, Martindale RG, Leibach FH, Ganapathy ME, Prasad PD, Ganapathy V. Structure, function, and tissue expression pattern of human SN2, a subtype of the amino acid transport system N. Biochem Biophys Res Commun. 2001; 281(5):1343–8. [PubMed: 11243884]
40. Fei YJ, Sugawara M, Nakanishi T, Huang W, Wang H, Prasad PD, Leibach FH, Ganapathy V. Primary structure, genomic organization, and functional and electrogenic characteristics of human system N 1, a Na+- and H+-coupled glutamine transporter. J Biol Chem. 2000; 275(31):23707–17. [PubMed: 10823827]

41. Hatanaka T, Huang W, Ling R, Prasad PD, Sugawara M, Leibach FH, Ganapathy V. Evidence for the transport of neutral as well as cationic amino acids by ATA3, a novel and liver-specific subtype of amino acid transport system A. Biochim Biophys Acta. 2001; 1510(1–2):10–7. [PubMed: 11342143]

42. Zaia KA, Reimer RJ. Synaptic Vesicle Protein NTT4/XT1 (SLC6A17) Catalyzes Na+-coupled Neutral Amino Acid Transport. J Biol Chem. 2009; 284(13):8439–48. [PubMed: 19147495]

43. Parra LA, Baust T, Mestikawy SE, Quiroz M, Hoffman B, Haflett JM, Yao JK, Torres GE. The Orphan Transporter Rxt1/NTT4 (SLC6A17) Functions as a Synaptic Vesicle Amino Acid Transporter Selective for Proline, Glycine, Leucine, and Alanine. Mol Pharmacol. 2008; 74(6): 1521–32. [PubMed: 18768736]

44. Carl SM, Lindley DJ, Das D, Couraud PO, Weksler BB, Romero I, Mowery SA, Knipp GT. ABC and SLC transporter expression and proton oligopeptide transporter (POT) mediated permeation across the human blood--brain barrier cell line, hCMEC/D3 [corrected]. Mol Pharm. 2010; 7(4): 1057–68. [PubMed: 20524699]

45. Schinkel AH, Smit JJ, van Tellingen O, Beijnen JH, Wagenaar E, van Deemter L, Mol CA, van der Valk MA, Robanus-Maandag EC, te Riele HP. Disruption of the mouse mdr1a P-glycoprotein gene leads to a deficiency in the blood-brain barrier and to increased sensitivity to drugs. Cell. 1994; 77(4):491–502. [PubMed: 7910522]

46. Jonker JW, Buitelaar M, Wagenaar E, van der Valk MA, Scheffer GL, Scheper RJ, Plosch T, Kuipers F, Elferink RP, Rosing H, Beijnen JH, Schinkel AH. The breast cancer resistance protein protects against a major chlorophyll-derived dietary phototoxin and protoporphyria. Proc Natl Acad Sci U S A. 2002; 99(24):15649–54. [PubMed: 12429862]

47. YH, Shen H, Keep RF, Smith DE. Peptide transporter 2 (PEPT2) expression in brain protects against 5-aminolevulinic acid neurotoxicity. J Neurochem. 2007; 103(5):2058–65. [PubMed: 17854384]

48. Jiang H, Hu Y, Keep RF, Smith DE. Enhanced antinociceptive response to intracerebroventricular kyotorphin in Pept2 null mice. J Neurochem. 2009; 109(5):1536–43. [PubMed: 19383084]

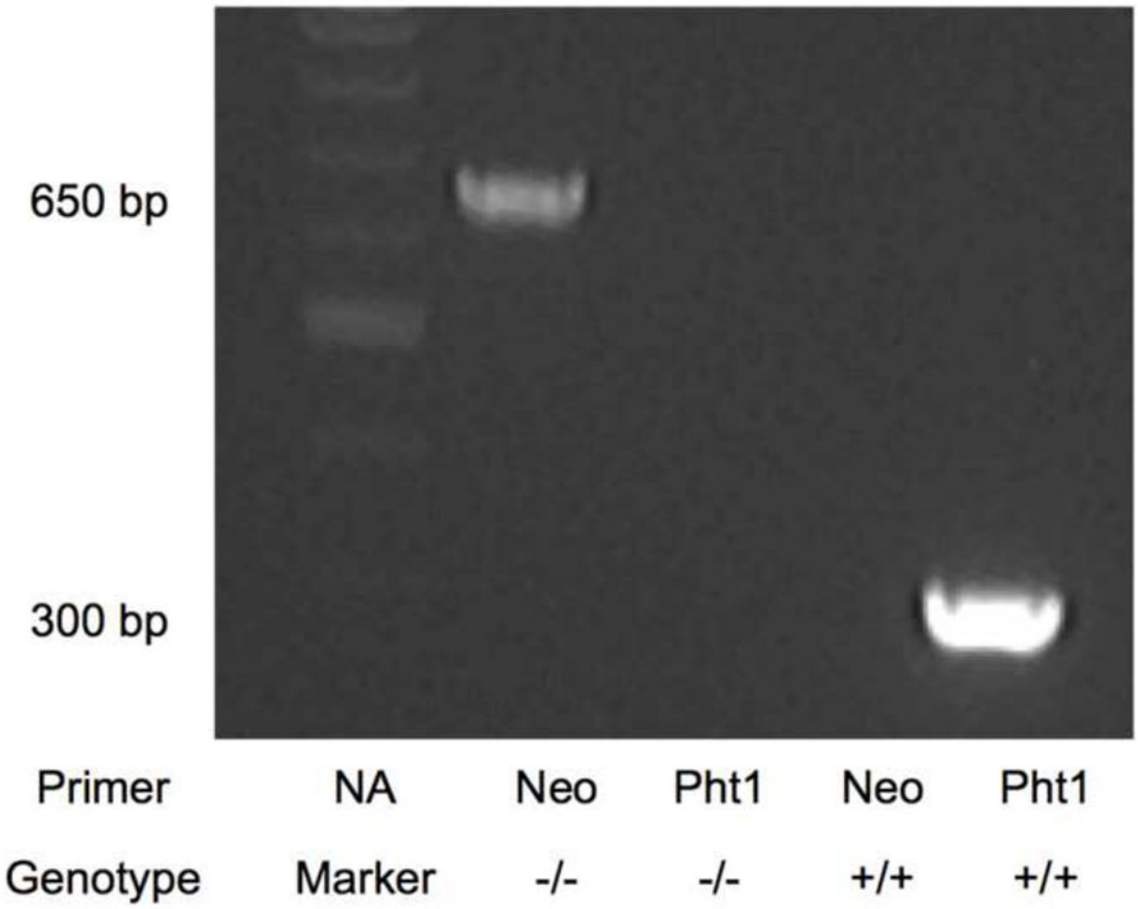

Figure 1.

Genotyping results for the identification of *Pht1* null mice. NA (Marker), gene-specific primer not applicable in DNA ladder consisting of 100 bp repeats; Neo (−/−), neomycin-specific primer in *Pht1* null mice; *Pht1* (−/−), *Pht1* gene-specific primer in *Pht1* null mice; Neo (+/+), neomycin-specific primer in wildtype mice; *Pht1* (+/+), *Pht1*-specific primer in wildtype mice.

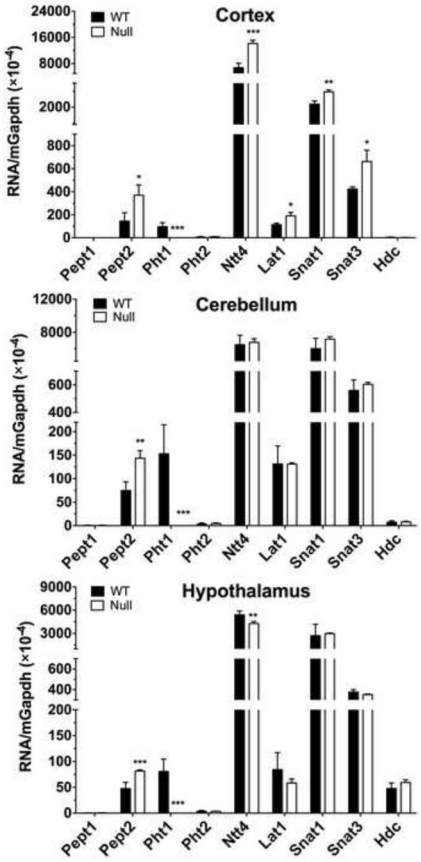

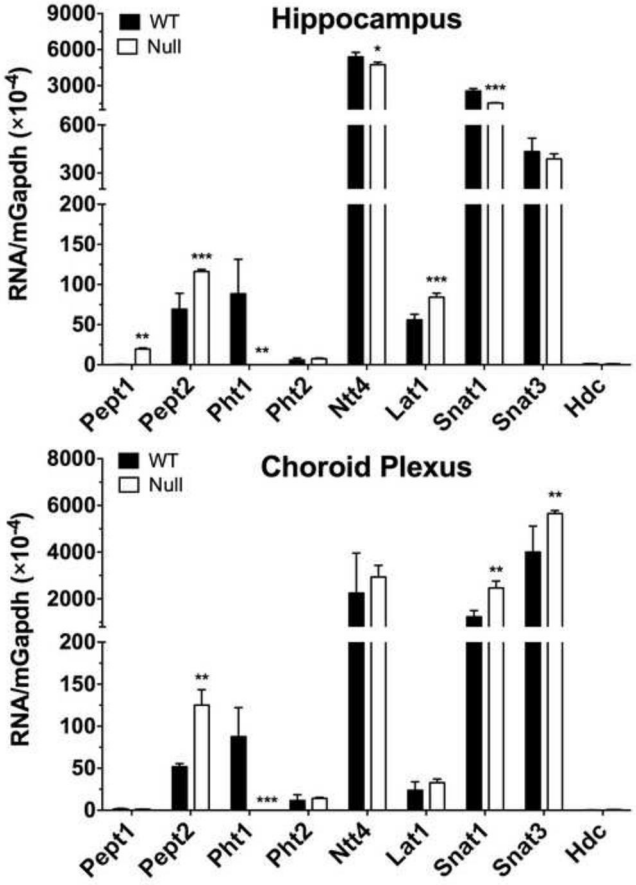

Figure 2.

mRNA expression of POTs (*Pept1, Pept2, Pht1, Pht2*), select amino acid transporters (*Ntt4, lat1, Snat1, Snat3*) and histidine decarboxylase (*Hdc*) in brain regions of adult wildtype (WT) and *Pht1* null mice (Null). Values are mean ± SE (n=4–6). *p≤0.05, **p≤0.01 and ***p≤0.001, as compared to WT mice, using a Student's t-test.

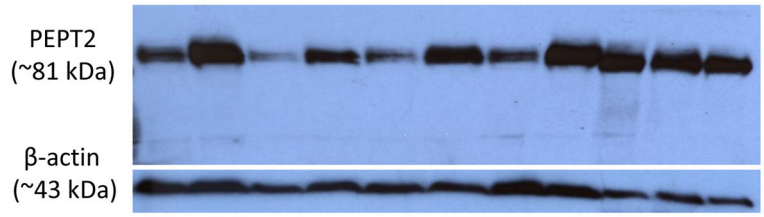

Genotype	-/-	+/+	-/-	+/+	-/-	+/+	-/-	+/+	-/-	+/+	+/+
Tissue	Cortex		Cereb		Hippo		Hypo		CP		Kid
Fold Change	1.71 (0.35)		1.58 (0.39)		2.76 (0.93)		4.78 (2.85)		1.61 (0.44)		NA

Figure 3.

Immunoblots of PEPT2 protein in cerebral Cortex, cerebellum (Cereb), hippocampus (Hippo), hypothalamus (Hypo) and choroid plexus (CP) of wildtype (+/+) and *Pht1* null (−/−) mice. β-Actin served as a loading control. Kidney (Kid) from wildtype mice was a positive control for PEPT2 protein. Fold change represents the expression ratio of β-actin-corrected PEPT2 protein in *Pht1* null mice, as compared to WT animals (n=4). NA, not applicable.

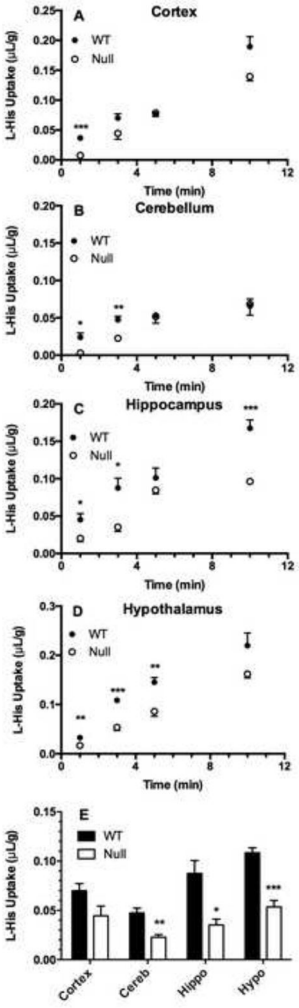

Figure 4.

Uptake of 2 μM L-[^{3}H]histidine in regional brain slices of adult wildtype (WT) and *Pht1* null (Null) mice as a function of time (A–D) and under initial-rate conditions (i.e., 3-min incubation) (E). Values are mean ± SE (n = 4). *p≤0.05, **p≤0.01 and ***p≤0.001, as compared to WT mice, using a Student's t-test.

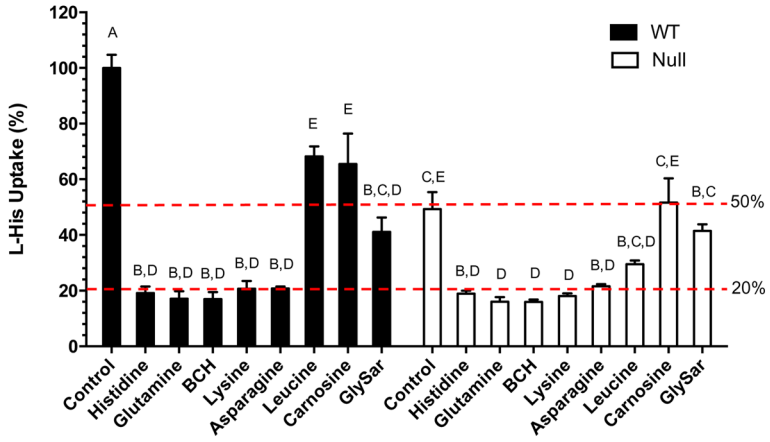

Figure 5.

Uptake of 2 μM L-[^{3}H]histidine at 3 min in hypothalamus slices of adult wildtype (WT) and *Pht1* null (Null) mice in the absence (control) or presence of potential inhibitors (5 mM). Values are mean ± SE (n=4). All treatment groups were compared, regardless of genotype, and those treatments with the same capital letter (i.e., A, B, C, D, or E) were not significantly different from one another. BCH, 2-aminobicyclo [2.2.1]heptane-2-carboxylic acid; GlySar, glycylsarcosine.

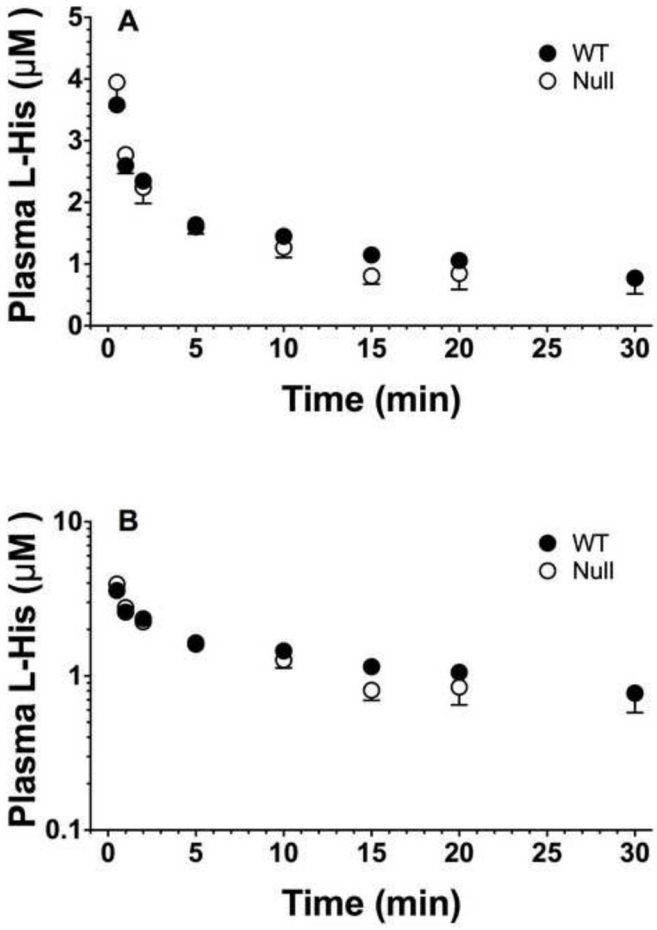

Figure 6.

Plasma concentration-time profiles of L-[^{14}C]histidine in wildtype (WT) and *Pht1* null (Null) mice after 1 nmol/g intravenous bolus dose. Data are expressed as mean ± SE (n=11 for WT and 12 for Null) in which the y-axis is displayed on a linear scale (A) and on a logarithmic scale (B).

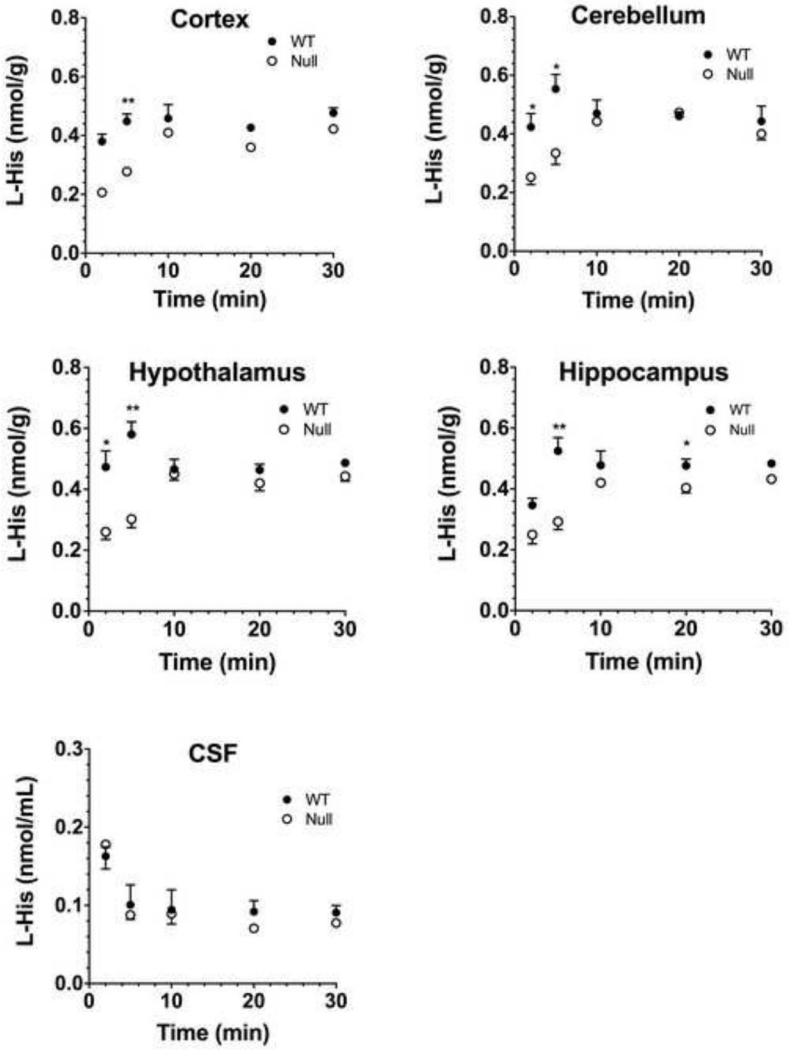

Figure 7.

Tissue and cerebrospinal fluid (CSF) concentrations of L-[^{14}C]histidine in brain regions of wildtype (WT) and *Pht1* null (Null) mice after 1 nmol/g intravenous bolus dose. Data are expressed as mean ± SE (n = 3–6). *p < 0.05 and **p < 0.01, as compared to WT mice, using a Student's t-test.

Table 1

Quantitative real-time PCR primers in mouse

Gene	Forward Primer (5′-3′)	Reverse Primer (5′-3′)
Pht1 (Slc15a4)	AGCTTTTTCACAGGCTACCTGATT	AGGCTTGGTGATGAAGACACTCT
Pht2 (Slc15a3)	GCTGAAGCTTGCGTTCCAA	AACAGGTGGGCACTTTCAGAGT
Pept1 (Slc15a1)	CCACGGCCATTTACCATACG	TGCGATCAGAGCTCCAAGAA
Pept2 (Slc15a2)	TGCAGAGGCACGGACTAGATAC	GGGTGTGATGAACGTAGAAATCAA
Lat1 (Slc7a5)	GGATGCCCATCTGTAGGTTTTTAT	AAAATAGAAAGCACTGGGCAAAAT
Snat1 (Slc38a1)	GCAGAACTCGACAGTCAGTGCTA	GCGATGGTTGGTAAAGCATACA
Snat3 (Slc38a3)	GCTGCCCATATATACAGAGCTCAA	CAGCAATGGACAGGTTGGAGAT
Ntt4 (Slc6a17)	ACGATGAGACGCGCTTCAT	AGCGTCCGTTGGGATTGTT
Hdc	AACCCCATCTACCTCCGACAT	GGGATCTGCCAATGCATGA

Hdc, histidine decarboxylase.

Table 2

Body weight and serum clinical chemistry of wildtype and *Pht1* null mice[a]

Parameter	Wildtype mice	*Pht1* null mice
Body weight		
7–8 weeks (g)		
Male	24.1 ± 0.5 (9)	23.2 ± 1.0 (9)
Female	18.6 ± 0.4 (12)	18.5 ± 0.3 (10)
Serum		
Sodium (mmol/L)	138 ± 3 (5)	140 ± 4 (6)
Potassium (mmol/L)	9.4 ± 3.0 (5)	9.2 ± 3.7 (6)
Chloride (mmol/L)	111 ± 1 (5)	112 ± 2 (4)
Albumin (g/dL)	3.9 ± 0.5 (6)	4.5 ± 0.9 (6)
Protein (g/dL)	8.2 ± 1.9 (6)	6.7 ± 1.5 (5)
Creatinine (mg/dL)	0.33 ± 0.05 (5)	0.56 ± 0.34 (6)
Bilirubin (mg/dL)	0.10 ± 0 (5)	0.10 ± 0 (5)
Glucose (mg/dL)	178 ± 21 (6)	153 ± 31 (6)
Calcium (mg/dL)	9.2 ± 0.3 (5)	9.2 ± 0.3 (5)
BUN (mg/dL)	38 ± 2 (5)	35 ± 4 (6)
ALT (U/L)	53 ± 4 (5)	50 ± 3 (4)
ALP (U/L)	128 ± 13 (5)	124 ± 9 (5)
AST (U/L)	185 ± 53 (5)	181 ± 20 (6)

[a]Data are expressed as mean ± SE (number of mice). BUN, urea nitrogen; ALT, alanine aminotransferase; ALP, alkaline phosphates; and AST, aspartate aminotransferase. No statistical differences were observed between the two genotypes, as determined by a Student's t-test.

Table 3

Noncompartmental pharmacokinetic analysis of [^{14}C]L-histidine in wildtype (WT) and *Pht1* null (Null) mice after 1 nmol/g intravenous bolus dose

Parameter	Unit	WT	Null
AUC_{0-30}	μM*min	21.7 (4.8)	24.6 (4.7)
$AUC_{0-\infty}$	μM*min	42.0 (8.0)	43.4 (6.3)
CL	mL/min	0.71 (0.15)	0.59 (0.10)
V_{ss}	mL	8.4 (0.7)	7.5 (0.7)
$t_{1/2}$	min	13.3 (3.8)	11.1 (1.6)
λ_z	min^{-1}	0.084 (0.015)	0.083 (0.014)
MRT	min	17.9 (4.6)	15.7 (2.3)

Data are expressed as mean (± SE) (n=11 for WT and 12 for *Pht1* null mice). No significant differences were observed between the two genotypes, as determined by a Student's t-test.